Psychiatry Research: Neuroimaging 292 (2019) 47–53

Contents lists available at ScienceDirect

Psychiatry Research: Neuroimaging

journal homepage: www.elsevier.com/locate/psychresns

Entorhinal cortex volume, thickness, surface area and curvature trajectories over the adult lifespan

Wang Yanpei[a,b], Hao Lei[a,b], Zhang Yuning[a,b,c], Zuo Chenyi[d,*], Wang Daoyang[d,*]

[a] State Key Laboratory of Cognitive Neuroscience and Learning, Beijing Normal University, Beijing, China
[b] IDG/McGovern Institute for Brain Research, Beijing Normal University, Beijing, China
[c] Institute of Psychiatry, Psychology, & Neurosciences, King's College London, London, UK
[d] College of Educational Science, Anhui Normal University, Wuhu, China

ARTICLE INFO

Keywords:
Entorhinal cortex
Volume
Thickness
Surface
Curvature
Aging

ABSTRACT

The entorhinal cortex (ERC) acts as a connection between the hippocampus and temporal cortex and plays a key role in memory retrieval and navigation. The morphology of this brain region changes with age. However, there are few quantitative magnetic resonance imaging studies of ERC morphology across the healthy adult lifespan. In this study, we quantified ERC volume, thickness, surface area, and curvature in a large number of subjects spanning seven decades of life. Using structural MRI data from 563 healthy subjects ranging from 19 to 86 years of age, we explored the adult lifespan trajectory of ERC volume, thickness, surface and curvature. ERC volume, thickness, and surface area initially increased with age, reaching a peak at about 32 years, 40 years, and 50 years of age, respectively, after which they decreased with age. ERC volume and surface area were hemispherically leftward asymmetric, whereas ERC thickness was hemispherically rightward asymmetric, with no gender differences. The direction of asymmetry differed across the measures. This informs previous inconsistencies in reports of ERC asymmetry. ERC aging began in mid-adulthood. At this stage of life, it may be important to adopt some strategies to reduce the effects of aging on cognition.

1. Introduction

With an aging population, it is very important to better understand the biomarkers of aging. In this respect, the brain has been found to be a stable predictor for aging (Lemaitre et al., 2012). Features of some cortical structures, such as the entorhinal cortex (ERC), have been identified as potential early biological markers of aging and Alzheimer's disease (AD) (Donix et al., 2013; Fischl et al., 2009; Morrison and Hof, 1997).

The ERC connects the temporal cortex and the deep arcuate cortex, such as the hippocampus (Fischl et al., 2009; Morrison and Hof, 1997). ERC tissue loss that occurs with age is an important marker of early cognitive and degenerative diseases, such as AD (Donix et al., 2013; Kochunov et al., 2011). Among all brain regions, the ERC provided the best resolution between cognitively intact individuals and patients with mild cognitive impairment (MCI) or AD (Whitwell et al., 2012). AD-induced cortex thinning was most evident in the medial temporal cortex of the rostral side (Dickerson et al., 2008). ERC volume was a powerful predictor of cognitive decline, including MCI and early AD (Cho et al., 2012; Varon et al., 2015). Larger ERC volume was associated with better memory in individuals with AD (Guzman et al., 2013). In addition, anxiety in AD indicates a larger rate of decline in ERC volume (Mah et al., 2015). However, cortical volume is only a summary statistic of a three-dimensional spatial structure, and ignores other aspects of the structure, such as the thickness, surface area, and curvature of the cerebral cortex, all of which vary with age (Khan et al., 2014). More directly, it is relatively unlikely that changes in cortical volume will not lead to simultaneous changes in the shape of the structure, and it is unlikely that a structure keeps the same general shape but only scales down in size (Madan, 2018). Consequently, any individual characteristics associated with volume differences, such as aging or neurodegenerative diseases, may take into account both volume and morphological characteristics. A more detailed understanding of the changes in cortical volume, thickness, surface area, and curvature of the ERC over the whole life cycle will further our understanding of the role of the ERC in neurodegeneration and natural aging.

Asymmetry plays a key role in brain information process (Kong et al., 2018; Liu et al., 2016). Among studies focousing on ERC asymmetry (Hasan et al., 2016; Simic et al., 2005), Simic et al. found that the ERC volume was leftward asymmetric whearas Hasan et al. reported the

* Corresponding authors.
E-mail addresses: zcy9461@163.com (C. Zuo), daoyangwang@126.com (D. Wang).

https://doi.org/10.1016/j.pscychresns.2019.09.002
Received 13 May 2019; Received in revised form 30 August 2019; Accepted 5 September 2019
Available online 06 September 2019

Table 1
Sample characteristics in different age groups.

Age group (year)	No. subjects	No.subjects 1/2/3 site[a]	Females(%)	Caucasian(%)	Education[b] mean(SD)
19–29	101	41/18/42	56(55.4)	70(69.3)	4.44(1.28)
30–39	99	50/22/27	39(39.4)	75(75.8)	4.55(1.05)
40–49	89	53/11/25	48(53.9)	75(84.3)	4.03(1.36)
50–59	99	65/3/31	61(61.6)	81(81.8)	3.46(1.50)
60–69	118	70/7/41	72(61.0)	98(83.1)	3.55(1.58)
70–79	49	29/6/14	34(69.4)	44(89.8)	3.39(1.57)
80–86	8	6/1/1	3(37.5)	8(100)	3.50(2.07)
Total	563	314/68/181	313(55.6)	451(80.1)	3.93(1.47)

[a] Three separate subsamples form different scanning sites in London: Guys Hospital Philips 1.5T/Institute of Psychiatry General Electric 1.5T/ Hammersmith Hospital with a Philips 3T scanner.
[b] Education levels: 1 = no qualifications; 2 = *O*-levels, GCSEs, or CSE; 3 = *A*-levels; 4 = further education; 5 = university or polytechnic degrees. SD, standard deviation.

ERC thickness was rightward asymmetric in the ERC thickness. We thought that this might be due to differences in the measures of two studies. Therefore, we analyzed the asymmetry in ERC volume, thickness, surface area and curvature.

There are few quantitative studies of ERC geometry measurements in healthy adults and throughout the adult lifespan (Fjell et al., 2014). The aim of this study was to fill this knowledge gap by quantifying ERC morphology across the adult lifespan. Our data provide, for the first time, a common gage of ERC volume, thickness, surface area, and curvature with age, sex, and lateralization.

2. Materials and methods

2.1. Participants

Data were obtained from the IXI database, which is an open-access, publicly available database containing T1-, T2-, and diffusion-weighted images from normal healthy subjects (http://www.brain-development.org) (Ziegler et al., 2012). ERC volume, thickness, surface area, and curvature were quantified from high-spatial-resolution T1-weighted magnetic resonance images from 563 individuals (250 males and 313 females) with a wide age distribution (aged 19–86 years), detailed in Table 1.

Tables 2 and 3.

2.2. Anatomical magnetic resonance image data processing

The processing pipeline used is described here in brief, and a more detailed description is available elsewhere (Tustison et al., 2014). Cortical volume, thickness, surface area, and curvature were quantified from the T1-weighted images using FreeSurfer software (version 6.0.0; http://surfer.nmr.mgh.harvard.edu/) (Fischl et al., 2009). After visual inspection to rule out artifacts, T1-weighted images were automatically segmented into cortical, subcortical gray and white matter, and cerebrospinal fluid. Based on cortical atlas labels, FreeSurfer software provided the mean thickness, surface area, and curvature of the cortex (http://www.freesurfer.net/fswiki/CorticalParcellation) (Desikan et al., 2006), which included ERC volume, thickness, surface area, and curvature.

2.3. Statistical analysis

All statistical analyses were conducted using SPSS 23.0 software (Chicago, IL). Group comparisons (left hemisphere vs. right hemisphere and males vs. females) were performed using paired *t*-tests. Linear and non-linear regressions were used to estimate the effects of age and sex on ERC volume, thickness, surface area, and curvature from the quadratic model to linear model, including the main effects of sex and age and the interaction of sex and age (Narvacan et al., 2017). Each ERC measure was fitted to (i) Quadratic: ERC = Intercept + A(Sex) + B(Age) + C(Age^2) + D(Age × Sex) + E(Age^2 × Sex) + residual error; or (ii) Linear: ERC = Intercept + A(Sex) + B(Age) + C(Age × Sex) + residual error. If the age and sex interaction was not significant, the ERC measure was re-fit with only main effects without interaction terms. For each measure, there were four fits to choose from. Akaike Information Criterion was used to compare models, and the fit with the lowest Akaike Information Criterion was selected as the best-fit model for the age trajectory (Tamnes et al., 2013). If a quadratic model was selected, age at peak was calculated from the first derivative. Statistical significance was set at $p < 0.05$, after adjusting for the number of comparisons (Fig. 1).

3. Results

3.1. Cortical volume

ERC volume increased with age until it reached a peak at about 40 years of age (41.29 years and 40.43 years in the left and right hemisphere, respectively), after which it decreased with age (Fig. 2A and Fig 2B). ERC volume was larger in males than in females ($p < 0.001$ for left and right hemispheres, controlling for whole brain volume, $p < 0.003$). The trajectory of ERC volume across the age span was similar in males and females with no significant age by sex interaction. ERC volume was leftward asymmetric, meaning that it was greater in the left hemisphere than in the right hemisphere ($p < 0.001$).

We then assessed ERC volume within narrow age ranges (Fig. 4A). ERC volume was leftward asymmetric in all age groups between 19 and 86 years (all $p < 0.05$; Fig. 4A). Left and right ERC cortical volume was strongly correlated in all age groups (all $r > 0.48$; $p < 0.05$). The rate of growth or atrophy with advancing age is shown in Fig. 3.

Table 2
Fitting parameters for ERC gray matter volume, thickness, surface and curvature versus age within each hemisphere.

Measures	Hem	Best fit model	Parameter(S.E.) Intercept[a]	Sex	Age	Age^2	Interaction (age*sex or age^2*sex)
Volume	left	Quadratic	800.10(71.76)	142.07(15.75)	10.24(3.12)	−0.124(0.032)	–
	right	Quadratic	732.25(68.81)	114.11(15.10)	6.30(2.99)	−0.078(0.030)	–
Thickness	left	Quadratic	2.73(0.13)	0.121(0.027)	0.015(0.005)	$-1.48(0.55)*10^{-4}$	–
	right	Quadratic	2.92(0.13)	0.126(0.029)	0.015(0.006)	$-1.55(0.58)*10^{-4}$	–
Surface	left	Quadratic	199.26(12.16)	22.77(2.67)	n. s.	−0.015(0.005)	–
	right	Quadratic	155.62(11.92)	17.10(2.62)	0.73(0.52)	−0.010(0.005)	–
Curvature	left	Quadratic	0.137(0.006)	0.004(0.001)	n. s.	$6.87(2.67)*10^{-6}$	–
	right	Quadratic	0.144(0.008)	0.004(0.002)	$-7.36(3.39)*10^{-4}$	$8.89(3.42)*10^{-4}$	–

– = not applicable; n.s. = non-significant; Hem = Hemisphere.
[a] Intercept is the extrapolated value at age zero.

Table 3
Entorhinal Cortical volume, thickness and surface average and standard deviation of the left and right entorhinal cortical volume, thickness, surface and curvature along with paired t-Test comparisons and percentage difference using multicenter data from healthy controls grouped for ages 19–29, 30–39, 40–49, 50–59, 60–69, 70–79, and 80–89 years.

Age Group (Years)	*n* (Females)	Measures	Left (Mean ± SD)	Right (Mean ± SD)	*p* (Left vs. Right)	[a]Difference (%)
19–29	101(56)	volume	1039.96 ± 217.94	901.40 ± 184.58	1.67×10^{-12}	15.37
		thickness	3.08 ± 0.36	3.26 ± 0.33	4.41×10^{-08}	−5.70
		surface	224.46 ± 36.48	175.89 ± 35.89	6.92×10^{-27}	27.61
		curvature	0.131 ± 0.017	0.134 ± 0.023	0.154	−2.35
30–39	99(39)	volume	1097.88 ± 183.77	914.76 ± 165.45	3.34×10^{-17}	20.02
		thickness	3.18 ± 0.29	3.33 ± 0.34	1.72×10^{-06}	−4.66
		surface	224.43 ± 36.65	174.26 ± 29.93	7.80×10^{-25}	28.79
		curvature	0.13 ± 0.014	0.131 ± 0.017	0.844	−0.25
40–49	89(48)	volume	1063.40 ± 199.80	910.29 ± 183.90	1.05×10^{-12}	16.82
		thickness	3.11 ± 0.27	3.23 ± 0.30	3.79×10^{-05}	−3.71
		surface	221.90 ± 32.85	182.22 ± 32.60	1.63×10^{-19}	21.77
		curvature	0.130 ± 0.015	0.131 ± 0.019	0.547	−0.92
50–59	99(61)	volume	1054.68 ± 191.43	882.98 ± 174.59	3.61×10^{-20}	19.45
		thickness	3.20 ± 0.31	3.32 ± 0.28	8.49×10^{-06}	−3.82
		surface	204.60 ± 27.03	163.17 ± 27.59	6.95×10^{-30}	25.39
		curvature	0.131 ± 0.013	0.132 ± 0.018	0.782	−0.41
60–69	118(72)	volume	996.18 ± 168.60	871.70 ± 189.51	1.04×10^{-12}	14.28
		thickness	3.17 ± 0.34	3.33 ± 0.34	1.61×10^{-09}	−5.05
		surface	204.60 ± 27.03	163.17 ± 27.59	6.95×10^{-30}	25.39
		curvature	0.134 ± 0.015	0.136 ± 0.02	0.191	−1.79
70–79	49(34)	volume	910.61 ± 235.72	793.08 ± 237.12	1.39×10^{-05}	14.82
		thickness	3.04 ± 0.38	3.13 ± 0.49	0.08	−2.77
		surface	194.04 ± 28.50	160.20 ± 29.69	1.89×10^{-09}	21.12
		curvature	0.141 ± 0.021	0.143 ± 0.024	0.718	−1.07
80–86	8(3)	volume	912.25 ± 254.80	732.00 ± 166.57	0.02	24.62
		thickness	3.02 ± 0.39	2.94 ± 0.380	0.61	2.47
		surface	189.50 ± 21.72	158.88 ± 17.35	4.14×10^{-04}	19.28
		curvature	0.142 ± 0.016	0.138 ± 0.011	0.505	2.80

[a] Percentage Difference Between Right and Left (%).

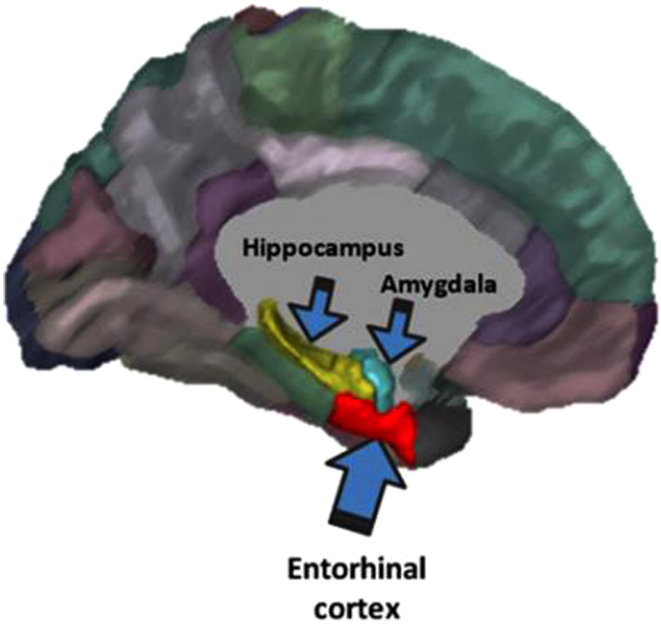

Fig. 1. Three-dimensional view of the human medial temporal lobe showing the ERC (Brodmann's area 28) with respect to hippocampus, and amygdala as anatomical landmark anterior to hippocampus.

3.2. Cortical thickness

ERC thickness increased with age until it reached a peak at about 50 years of age (51.37 years and 47.58 years in the left and right hemisphere, respectively), after which it decreased with age (Fig. 2C and Fig 2D). ERC thickness was larger in males than in females ($p < 0.001$ for left and right hemispheres). The trajectory of ERC thickness across the age span was similar in males and females with no significant age by sex interaction. ERC thickness was rightward asymmetric, meaning that it was greater in the right hemisphere than in the left ($p < 0.001$).

We then assessed ERC thickness within narrow age ranges (Fig. 4B). ERC thickness was rightward asymmetric in all age groups between 19 and 86 years (Fig. 4B). Left and right ERC thickness was strongly correlated in all age groups (all $r > 0.5$; $p < 0.05$). The rate of growth or atrophy with advancing age is shown in Fig. 3.

3.3. Cortical surface area

ERC surface area increased with age until it reached a peak in the early-to-mid-thirties (31.15 years and 35.18 years in the left and right hemisphere, respectively), after which it decreased with age (Fig. 2E and F). ERC surface area was larger in males than in females ($p < 0.001$ for left and right hemispheres). The trajectory of ERC thickness across the age span was similar in males and females with no significant age by sex interaction. ERC surface area was leftward asymmetric, meaning that it was greater in the left hemisphere than in the right ($p < 0.001$).

We then assessed ERC surface area within narrow age ranges (Fig. 4C). ERC surface area was leftward asymmetric in all age groups between 19 and 86 years (all $p < 0.05$; Fig. 4C). Left and right ERC surface area was strongly correlated in all age groups (all $r > 0.39$; $p < 0.05$). The rate of growth or atrophy with advancing age is shown in Fig. 3.

3.4. Cortical curvature

ERC curvature decreased with age until it reached a nadir at about 40 years of age (36.98 years and 41.39 years in the left and right hemisphere, respectively), after which it increased with age (Fig. 2G and H). ERC curvature was larger in males than in females (left: $p = 0.013$; right: $p = 0.024$). The trajectory of ERC curvature across the age span was similar in males and females, with no significant sex effect

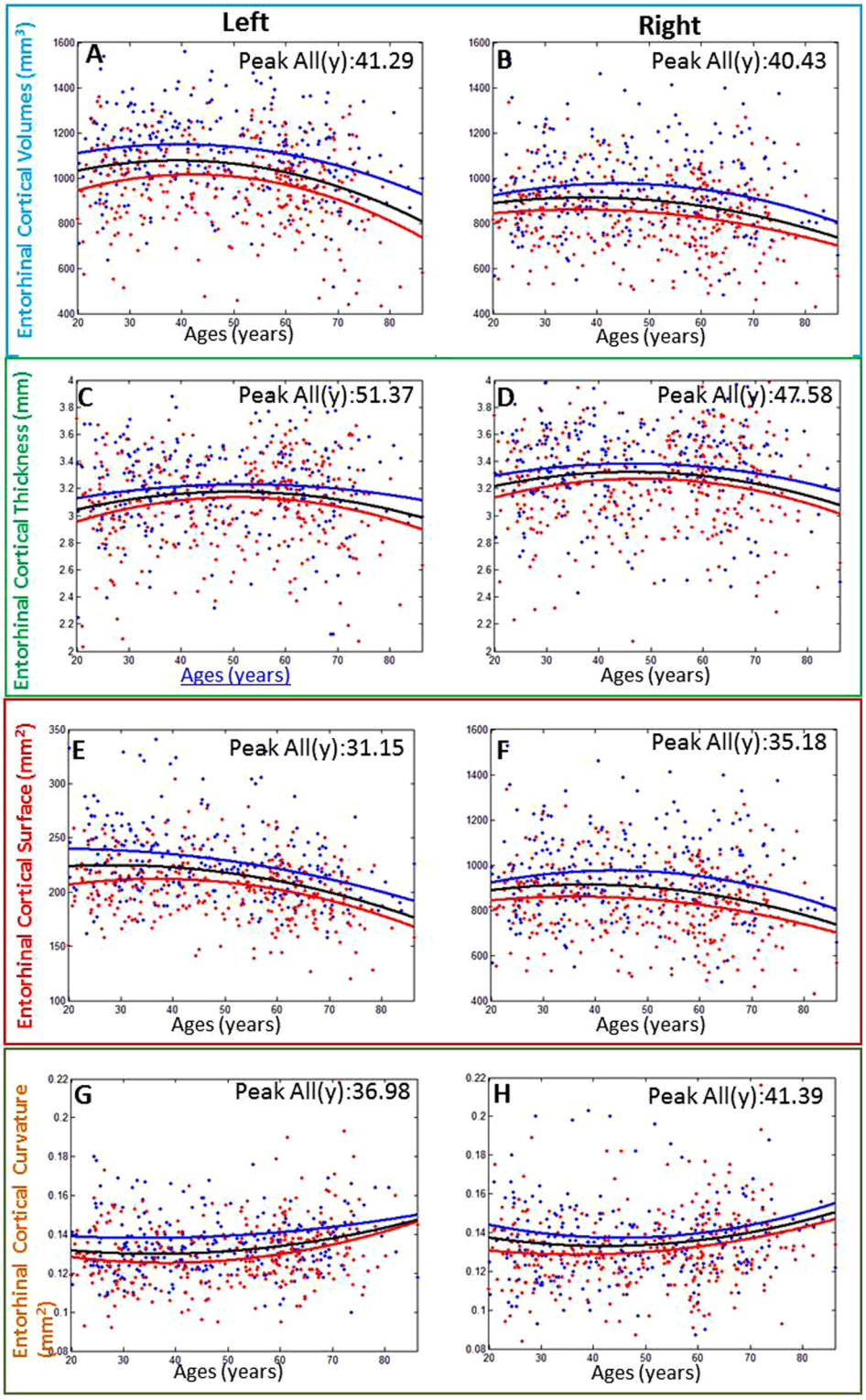

Fig. 2. The trajectories of left and right ERC cortical volumes (A, B), thickness (C, D), surface (E, F) and curvature (G, H). Note that males (blue lines) and females (red lines) showed very similar age trajectories with no significant age by sex interactions, although males had significantly larger cortical volumes, thickness, surface and curvature across the age span (all $p < 0.05$).

and age by sex interaction. ERC curvature had no asymmetry, being similar in the left and right hemispheres ($p = 0.083$).

We then assessed ERC curvature within narrow age ranges (Fig. 4D). ERC curvature had no asymmetry in any age group between 19 and 86 years (all $p > 0.15$; Fig. 4D). The rate of growth or atrophy with advancing age is shown in Fig. 3.

4. Discussion

This study used a large number of samples collected as part of the UK health-controlled open-access data set (IXI database) to quantify the trajectories of ERC gray matter volume, thickness, surface area, and curvature across the lifespan. Consistent with previous studies, we did

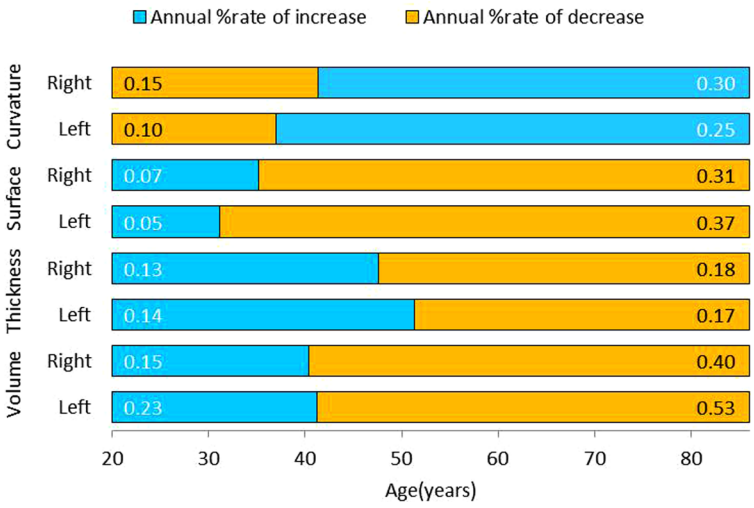

Fig. 3. Relative timing and magnitude of volumetric changes within the adults lifespan. The magnitude of the annual increase or decrease in percentage volume is shown for each measure. Blue bars denote increases of volume before peak age, while orange bars indicate decreases. Cortical volume, thickness and surface are arranged by increasing age at peak value, while curvature was inverted. Each measure of ERC reach peak at different ages, with the surface peaking earlier than the thickness and gray matter volume.

not find a gender by age interaction in any outcome measure (Grieve et al., 2011), and all measures followed a quadratic trajectory with age.

Previous reports on the symmetry of the ERC are inconsistent. Hasan et al. reported that the ERC was hemispherically rightward asymmetric (Hasan et al., 2016). However, an earlier postmortem-based study reported that the volume and surface area of the verrucae part of the ERC were greater in the left hemisphere than in the right, and this leftward asymmetry was highly significant (Simic et al., 2005). These authors also reported that the neuron number estimated by the optical fractionator was not significantly different between the two hemispheres (Simic et al., 2005). Hasan et al. ascribed the cause of this difference to differences in analysis technique (postmortem vs. in vivo imaging) and the region of interest (ERC verrucae vs. global ERC) (Hasan et al., 2016). The results of the current study suggest that the discrepancy may be due to the different measures used. We found that ERC thickness was rightward asymmetric whereas volume and surface area were leftward asymmetric.

The asymmetry may be related to the role of the ERC. The medial ERC receives inputs from the superior temporal gyrus, and the lateral ERC receives inputs from the parainsular cortex (Insausti et al., 1987). The superior temporal gyrus, the parainsular cortex, and Broca's motor-speech area are leftward asymmetric (Amunts et al., 2003). The ERC is a gateway between the hippocampus and the neocortex, and plays an important role in the process of memory and learning (Eichenbaum, 2000). Therefore, we speculate that the leftward asymmetry of ERC volume and surface area may play a role in memory processing of language in the left hemisphere. This also explains the dominance of the left hippocampus over the right in its capacity for verbal episodic memory (Kelley et al., 1998). Based on a patient with anterior temporal injury that included the ERC and hippocampus, Tranel proposed that the left hemisphere ERC was more involved in verbal processing and the right hemisphere ERC in non-verbal processing (Tranel, 1991). This was supported by a follow-up study in which the authors found that disruption of the left ERC caused verbal episodic memory deficit (Eustache et al., 2001). In individuals with AD, decreased memory verbal performance was associated with an increased rate of ERC atrophy, especially in the left hemisphere (Du et al., 2003). We observed that ERC thickness was hemispherically rightward asymmetric in males and females. This suggests that the ERC thickness is involved in non-verbal processing. ERC thickness, which plays a key role in spatial skills (Mendoza and Foundas, 2007), is greatest in the right hemisphere, which is the dominant hemisphere for spatial memory and orientation. ERC asymmetry is reduced in individuals with MCI (Long et al., 2013) or AD (Thompson et al., 2003). The early onset of asymmetric loss in the ERC has potential as a biological marker for early identification of MCI (Dickerson, 2007), as it was identified as the first time the tissue loss and neurofibrillary tangle histologically (van der Flier et al., 2011), along with functional degeneration in individuals with MCI or AD (Devanand et al., 2007). An early lack of asymmetry in the ERC and the loss of the laterality shift in the limbic system have been suggested as biological markers to identify preclinical AD (Long et al., 2013).

Our finding of an earlier and faster decrease in right ERC thickness is consistent with that of a recent study. ERC volume and surface area decreased earlier and faster in the left hemisphere than in the right hemisphere, whereas volume decreased simultaneously in the left and right hemispheres. ERC curvature did not show any lateralization and initially increased with aging. Curvature is an indicator of cortex complexity, and the increase in curvature with age may indicate that people's experience is still growing as they age.

Of the three measures that increased to a peak and then decreased with age, ERC surface area was the first to decline, with the peak occurring at around 32 years of age. This was followed by volume (peak at 40 years of age) and then thickness (peak at around 50 years of age). A decline in surface area may be the first sign that the ERC has begun to age. We speculate that the different trajectories of these three measures across the adult lifespan may be helpful to identify in vivo patterns of defects in cognitive and degenerative diseases such as MCI and AD (Mendoza and Foundas, 2007). The pattern of rise-plateau-decrease observed in ERC volume, surface area, and thickness mimics the results of histological studies on synaptic (Huttenlocher and Dabholkar, 1997) and dendrite tree density (Petanjek et al., 2008) in humans. Interestingly, ERC curvature shows the opposite pattern, i.e., decrease-plateau-rise. A previous study (Wang et al., 2014) have reported that cortical curvature is sensitive to changes induced by aging. This study is the first to show that ERC curvature could be a key marker of aging.

5. Limitations

The present study has limitations that should be mentioned. First, our findings are derived from cross-sectional data and are not longitudinal observations. As such, they do not take individual differences in the aging process into account. Second, due to a lack of psychometric data, we could not evaluate any relations between ERC aging and cognitive or behavioral performance.

6. Conclusions

The present study explored the trajectory of ERC volume, thickness, surface area, and curvature across the adult lifespan and the asymmetry of these measures across the two hemispheres across the lifespan. We

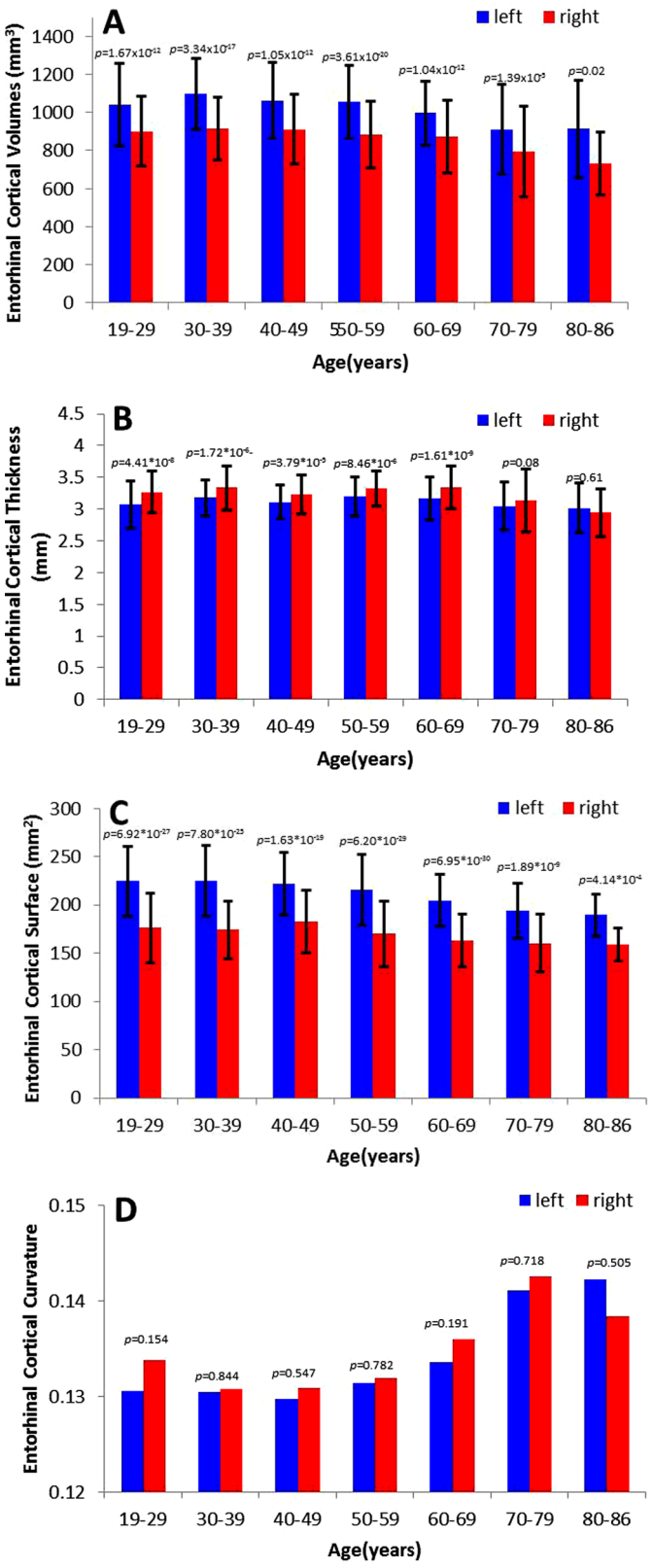

Fig. 4. Bar plots showing average and standard deviation of the left (blue) and right (red) entorhinal cortical volumes (A), thickness (B), surface (C) and curvature (D) along with paired *t*-test comparisons using data grouped for ages 19–29, 30–39, 40–49, 50–59, 60–69, 70–79, and 80–89 years. Left volumes, thickness and surface were larger than right significantly, but no difference was found in curvature.

found that asymmetry differed across the different measures, with thickness displaying rightward asymmetry and volume and surface area displaying leftward asymmetry. These results address inconsistencies in previous reports of ERC asymmetry. The reported trajectory of these four measures across the adult lifespan can provide a normative baseline for patient studies and studies targeting biological markers and environmental modulators of ERC volume, thickness, surface area, and curvature with aging (Grieve et al., 2011; Kochunov et al., 2011). Our results suggest that ERC aging (manifest as volume atrophy, cortical thinning, surface area shrinkage and curvature increased) begins to occur in middle adulthood. At this stage of life, it may be important to adopt some strategies to reduce the effects of aging on cognition.

Acknowledgments

This work was supported by a grant from The key Projects for Natural Science Research in Colleges and Universities in Anhui Province: The Brain Mechanism of the Development of Children's Adolescents' Creative Ability and Its Interaction with Gene-Environment (grant number: KJ2018A0306).

References

Amunts, K., Schleicher, A., Ditterich, A., Zilles, K., 2003. Broca's region: cytoarchitectonic asymmetry and developmental changes. J. Comp. Neurol. 465, 72–89.
Cho, Y., Seong, J.K., Jeong, Y., Shin, S.Y., Neuroimaging, A.D., 2012. Individual subject classification for Alzheimer's disease based on incremental learning using a spatial frequency representation of cortical thickness data. Neuroimage 59, 2217–2230.
Desikan, R.S., Segonne, F., Fischl, B., Quinn, B.T., Dickerson, B.C., Blacker, D., Buckner, R.L., Dale, A.M., Maguire, R.P., Hyman, B.T., Albert, M.S., Killiany, R.J., 2006. An automated labeling system for subdividing the human cerebral cortex on MRI scans into gyral based regions of interest. Neuroimage 31, 968–980.
Devanand, D.P., Pradhaban, G., Liu, X., Khandji, A., De Santi, S., Segal, S., Rusinek, H., Pelton, G.H., Honig, L.S., Mayeux, R., Stern, Y., Tabert, M.H., de Leon, M.J., 2007. Hippocampal and entorhinal atrophy in mild cognitive impairment: prediction of Alzheimer disease. Neurology 68, 828–836.
Dickerson, B.C., 2007. The entorhinal cortex: an anatomical mediator of genetic vulnerability to Alzheimer's disease? Lancet Neurol. 6, 471–473.
Dickerson, B.C., Bakkour, A., Salat, D.H., Feczko, E., Pacheco, J., Greve, D.N., Grodstein, F., Wright, C.I., Blacker, D., Rosas, H.D., 2008. The cortical signature of Alzheimer's disease: regionally specific cortical thinning relates to symptom severity in very mild to mild AD dementia and is detectable in asymptomatic amyloid-positive individuals. Cereb. Cortex 19, 497–510.
Donix, M., Burggren, A.C., Scharf, M., Marschner, K., Suthana, N.A., Siddarth, P., Krupa, A.K., Jones, M., Martin-Harris, L., Ercoli, L.M., Miller, K.J., Werner, A., von Kummer, R., Sauer, C., Small, G.W., Holthoff, V.A., Bookheimer, S.Y., 2013. APOE associated hemispheric asymmetry of entorhinal cortical thickness in aging and Alzheimer's disease. Psychiat. Res. 214, 212–220.
Du, A.T., Schuff, N., Zhu, X.P., Jagust, W.J., Miller, B.L., Reed, B.R., Kramer, J.H., Mungas, D., Yaffe, K., Chui, H.C., Weiner, M.W., 2003. Atrophy rates of entorhinal cortex in Ad and normal aging. Neurology 60, 481–486.
Eichenbaum, H., 2000. A cortical–hippocampal system for declarative memory. Nat. Rev. Neurosci. 1, 41.
Eustache, F., Desgranges, B., Giffard, B., de la Sayette, V., Baron, J.C., 2001. Entorhinal cortex disruption causes memory deficit in early Alzheimer's disease as shown by PET. Neuroreport 12, 683–685.
Fischl, B., Stevens, A.A., Rajendran, N., Yeo, B.T., Greve, D.N., Van Leemput, K., Polimeni, J.R., Kakunoori, S., Buckner, R.L., Pacheco, J., Salat, D.H., Melcher, J., Frosch, M.P., Hyman, B.T., Grant, P.E., Rosen, B.R., van der Kouwe, A.J., Wiggins, G.C., Wald, L.L., Augustinack, J.C., 2009. Predicting the location of entorhinal cortex from MRI. Neuroimage 47, 8–17.
Fjell, A.M., Westlye, L.T., Grydeland, H., Amlien, I., Espeseth, T., Reinvang, I., Raz, N., Dale, A.M., Walhovd, K.B., Alzheimer Disease Neuroimaging, I., 2014. Accelerating cortical thinning: unique to dementia or universal in aging? Cereb. Cortex 24, 919–934.
Grieve, S.M., Korgaonkar, M.S., Clark, C.R., Williams, L.M., 2011. Regional heterogeneity in limbic maturational changes: evidence from integrating cortical thickness, volumetric and diffusion tensor imaging measures. Neuroimage 55, 868–879.
Guzman, V.A., Carmichael, O.T., Schwarz, C., Tosto, G., Zimmerman, M.E., Brickman, A.M., Initiative, A.s.D.N., 2013. White matter hyperintensities and amyloid are independently associated with entorhinal cortex volume among individuals with mild cognitive impairment. Alzheimers Dement 9, S124–S131.
Hasan, K.M., Mwangi, B., Cao, B., Keser, Z., Tustison, N.J., Kochunov, P., Frye, R.E., Savatic, M., Soares, J., 2016. Entorhinal cortex thickness across the human lifespan. J. Neuroimaging 26, 278–282.
Huttenlocher, P.R., Dabholkar, A.S., 1997. Regional differences in synaptogenesis in

human cerebral cortex. J. Comput. Neurosci. 387, 167–178.
Insausti, R., Amaral, D.G., Cowan, W.M., 1987. The entorhinal cortex of the monkey: II. Cortical afferents. J. Comput. Neurosci. 264, 356–395.
Kelley, W.M., Miezin, F.M., McDermott, K.B., Buckner, R.L., Raichle, M.E., Cohen, N.J., Ollinger, J.M., Akbudak, E., Conturo, T.E., Snyder, A.Z., Petersen, S.E., 1998. Hemispheric specialization in human dorsal frontal cortex and medial temporal lobe for verbal and nonverbal memory encoding. Neuron 20, 927–936.
Khan, U.A., Liu, L., Provenzano, F.A., Berman, D.E., Profaci, C.P., Sloan, R., Mayeux, R., Duff, K.E., Small, S.A., 2014. Molecular drivers and cortical spread of lateral entorhinal cortex dysfunction in preclinical Alzheimer's disease. Nat. Neurosci. 17, 304–311.
Kochunov, P., Glahn, D.C., Lancaster, J., Thompson, P.M., Kochunov, V., Rogers, B., Fox, P., Blangero, J., Williamson, D.E., 2011. Fractional anisotropy of cerebral white matter and thickness of cortical gray matter across the lifespan. Neuroimage 58, 41–49.
Kong, X.Z., Mathias, S.R., Guadalupe, T., Group, E.L.W., Glahn, D.C., Franke, B., Crivello, F., Tzourio-Mazoyer, N., Fisher, S.E., Thompson, P.M., Francks, C., 2018. Mapping cortical brain asymmetry in 17,141 healthy individuals worldwide via the ENIGMA Consortium. P. Natl. Acad. Sci. USA 115, E5154–E5163.
Lemaitre, H., Goldman, A.L., Sambataro, F., Verchinski, B.A., Meyer-Lindenberg, A., Weinberger, D.R., Mattay, V.S., 2012. Normal age-related brain morphometric changes: nonuniformity across cortical thickness, surface area and gray matter volume? Neurobiol. Aging 33, 617 e611-619.
Liu, W., Mao, Y., Wei, D., Yang, J., Du, X., Xie, P., Qiu, J., 2016. Structural asymmetry of dorsolateral prefrontal cortex correlates with depressive symptoms: evidence from healthy individuals and patients with major depressive disorder. Neurosci. Bull. 32, 217–226.
Long, X., Zhang, L., Liao, W., Jiang, C., Qiu, B., Alzheimer's Disease Neuroimaging, I., 2013. Distinct laterality alterations distinguish mild cognitive impairment and Alzheimer's disease from healthy aging: statistical parametric mapping with high resolution MRI. Hum. Brain Mapp. 34, 3400–3410.
Madan, C.R., 2018. Shape-related characteristics of age-related differences in subcortical structures. Aging Ment. Health. 1–11.
Mah, L., Binns, M.A., Steffens, D.C., Alzheimer's Disease Neuroimaging, I., 2015. Anxiety symptoms in amnestic mild cognitive impairment are associated with medial temporal atrophy and predict conversion to Alzheimer disease. Am. J. Geriatr. Psychiatry 23, 466–476.
Mendoza, J., Foundas, A., 2007. Clinical neuroanatomy: A Neurobehavioral Approach. Springer Science & Business Media.
Morrison, J.H., Hof, P.R., 1997. Life and death of neurons in the aging brain. Science 278, 412–419.
Narvacan, K., Treit, S., Camicioli, R., Martin, W., Beaulieu, C., 2017. Evolution of deep gray matter volume across the human lifespan. Hum. Brain Mapp. 38, 3771–3790.
Petanjek, Z., Judas, M., Kostovic, I., Uylings, H.B., 2008. Lifespan alterations of basal dendritic trees of pyramidal neurons in the human prefrontal cortex: a layer-specific pattern. Cereb. Cortex 18, 915–929.
Simic, G., Bexheti, S., Kelovic, Z., Kos, M., Grbic, K., Hof, P.R., Kostovic, I., 2005. Hemispheric asymmetry, modular variability and age-related changes in the human entorhinal cortex. Neuroscience 130, 911–925.
Tamnes, C.K., Walhovd, K.B., Dale, A.M., Ostby, Y., Grydeland, H., Richardson, G., Westlye, L.T., Roddey, J.C., Hagler Jr., D.J., Due-Tonnessen, P., Holland, D., Fjell, A.M., Alzheimer's Disease Neuroimaging, I., 2013. Brain development and aging: overlapping and unique patterns of change. Neuroimage 68, 63–74.
Thompson, P.M., Hayashi, K.M., de Zubicaray, G., Janke, A.L., Rose, S.E., Semple, J., Herman, D., Hong, M.S., Dittmer, S.S., Doddrell, D.M., Toga, A.W., 2003. Dynamics of gray matter loss in Alzheimer's disease. J. Neurosci. 23, 994–1005.
Tranel, D., 1991. Dissociated verbal and nonverbal retrieval and learning following left anterior temporal damage. Brain Cognition 15, 187–200.
Tustison, N.J., Cook, P.A., Klein, A., Song, G., Das, S.R., Duda, J.T., Kandel, B.M., van Strien, N., Stone, J.R., Gee, J.C., Avants, B.B., 2014. Large-scale evaluation of ANTs and FreeSurfer cortical thickness measurements. Neuroimage 99, 166–179.
van der Flier, W.M., Pijnenburg, Y.A., Fox, N.C., Scheltens, P., 2011. Early-onset versus late-onset alzheimer's disease: the case of the missing APOE ε4 allele. Lancet Neurol 10, 280–288.
Varon, D., Barker, W., Loewenstein, D., Greig, M., Bohorquez, A., Santos, I., Shen, Q., Harper, M., Vallejo-Luces, T., Duara, R., Alzheimer's Disease Neuroimaging, I., 2015. Visual rating and volumetric measurement of medial temporal atrophy in the Alzheimer's Disease Neuroimaging Initiative (ADNI) cohort: baseline diagnosis and the prediction of MCI outcome. Int. J. Geriatr. Psych. 30, 192–200.
Wang, J.Q., Li, W.J., Mao, W., Dai, D., Hua, J., He, H.G., 2014. Age estimation using cortical surface pattern combining thickness with curvatures. Med. Biol. Eng. Comput. 52, 331–341.
Whitwell, J.L., Wiste, H.J., Weigand, S.D., Rocca, W.A., Knopman, D.S., Roberts, R.O., Boeve, B.F., Petersen, R.C., Jack Jr., C.R., Alzheimer Disease Neuroimaging, I., 2012. Comparison of imaging biomarkers in the Alzheimer Disease Neuroimaging Initiative and the Mayo Clinic Study of Aging. Arch. Neurol. 69, 614–622.
Ziegler, G., Dahnke, R., Jancke, L., Yotter, R.A., May, A., Gaser, C., 2012. Brain structural trajectories over the adult lifespan. Hum. Brain Mapp. 33, 2377–2389.